ISSN 1814-4225 (print)
ISSN 2663-2012 (online)

UDC 004.942: 614:4 **doi: 10.32620/reks.2025.1.01**

Dmytro CHUMACHENKO[1, 2, 3]

[1]*National Aerospace University "Kharkiv Aviation Institute", Kharkiv, Ukraine*
[2]*Balsillie School of International Affairs, Waterloo, ON, Canada*
[3]*University of Waterloo, Waterloo, ON, Canada*

A THEORETICAL FRAMEWORK FOR AGENT-BASED MODELLING OF INFECTIOUS DISEASE DYNAMICS UNDER MISINFORMATION AND VACCINE HESITANCY

The relevance of this study stems from the growing importance of modelling not only the biological transmission of infectious diseases but also the behavioural and informational factors that shape real-world epidemic dynamics. The ***subject*** *of this research is the development of an agent-based simulation framework capable of capturing the complex interactions between epidemiological processes, vaccination behaviour, and misinformation propagation. This study proposes and evaluates a modular, theoretically grounded model that simulates the spread of infection while accounting for belief-driven decision-making and dynamic social influence. To achieve this, the* ***tasks*** *included analyzing the current state of agent-based epidemic models, formalizing a system architecture with cognitive and logistical subsystems, and conducting scenario-based simulations to explore the effects of misinformation and behavioural resistance on vaccination uptake and epidemic outcomes. The* ***methodology*** *is based on a discrete-time SEIRDV structure extended with agent-level belief states, social influence mechanisms, and dynamic vaccination decisions. The model was implemented in Python and tested through a case study simulating a COVID-like outbreak in a synthetic population. The* ***results*** *demonstrate that even modest behavioural resistance can significantly increase mortality and delay epidemic control, whereas counter-misinformation interventions, if applied early and at sufficient intensity, can improve vaccine coverage and reduce disease burden. The study* ***concludes*** *that integrating behavioural and informational dynamics into epidemic models provides a more realistic and policy-relevant tool for analyzing communication strategies, vaccine rollout scenarios, and public health interventions under uncertainty.*

Keywords: *epidemic model; epidemic process; epidemic simulation; simulation; agent-based simulation; misinformation; vaccine hesitancy.*

1. Introduction

The simulation of infectious diseases is critical for understanding and mitigating the spread of pathogens within populations. Traditional compartmental models, such as the Susceptible-Infectious-Recovered (SIR) framework, have provided foundational insights into disease dynamics by segmenting populations into distinct categories and analyzing their transitions [1]. However, these models often rely on homogeneous mixing assumptions and may not capture the complexities inherent in real-life interactions [2]. To address these limitations, agent-based models have emerged as a powerful alternative, enabling the representation of individual behaviours, heterogeneous interactions, and localized environmental factors that influence disease transmission [3].

The COVID-19 pandemic underscored the indispensable role of simulation models in informing public health strategies [4]. Early in the outbreak, models were pivotal in projecting infection trajectories, assessing healthcare system capacities, and evaluating the potential impact of non-pharmaceutical interventions (NPI) such as social distancing and lockdowns [5]. For instance, the Covasim model, an agent-based framework, was instrumental in simulating the effects of various policy decisions on disease spread and health outcomes, thereby guiding policymakers in crafting effective responses [6].

A significant challenge during the COVID-19 crisis was the proliferation of health-related misinformation, which adversely affected public compliance with health directives and vaccine uptake [7]. The World Health Organization (WHO) highlighted that misleading information can lead to increased misinterpretations of scientific evidence, heightened mental distress, and misallocation of health resources [8]. Such misinformation often fuel vaccine hesitancy, undermining efforts to achieve herd immunity and control disease spread.

The beliefs and perceptions surrounding vaccination play a crucial role in infectious disease

transmission dynamics. Studies have demonstrated that exposure to vaccine-related misinformation correlates with decreased vaccine acceptance and compliance with public health guidelines [9]. This hesitancy endangers individual health and compromises community protection, facilitating the resurgence of preventable diseases [10].

Agent-based modelling offers a nuanced approach to simulating the spread of infectious disease by capturing the diversity of individual behaviours and interactions within a population [11]. Unlike aggregate models, ABMs incorporate factors such as social networks, mobility patterns, and behavioral responses to interventions [12]. For example, an agent-based model developed to assess lockdown scenarios demonstrated the ability to simulate disease spread within an abstract city, accounting for various places and agent types and aligning closely with observed infection patterns during the initial COVID-19 wave in Germany [13].

Incorporating misinformation dissemination, vaccination perceptions, and policy interventions into ABMs enhance their realism and applicability. By modelling the interplay between disease dynamics and information spread, researchers can better understand how false beliefs propagate and influence health behaviours. This integrated approach is vital for designing effective communication strategies and intervention policies to mitigate the impact of the disease and the accompanying infodemic.

This study **aims** to develop and theoretically ground a modular, agent-based simulation model that captures the complex dynamics of infectious disease spread. The model incorporates epidemiological transitions, individual behavioural responses, misinformation propagation, vaccine perceptions, supply logistics, and policy interventions, and it will be specifically applied to the COVID-19 pandemic.

To achieve this objective, the following **tasks** were formulated:

1. To comprehensively review existing agent-based models for infectious disease simulation, focusing on their strengths, limitations, and applicability in pandemic scenarios.

2. To develop a multi-layered agent-based model that integrates epidemiological, behavioural, informational, and logistic subsystems to simulate COVID-19 transmission in a socially heterogeneous population.

3. To develop a model of individual-level heterogeneity in vaccination decisions by accounting for cognitive dispositions, misinformation exposure, peer influence, and sociological clustering.

4. To develop the propagation model of health-related misinformation and its impact on vaccination willingness and public health behaviours using network-based belief dynamics and exogenous informational shocks.

5. To incorporate vaccine supply constraints and policy interventions into decision-making by simulating real-world limitations, such as dose availability, prioritization policies, and behavioural dropout risks.

6. To evaluate the interaction between subsystems and their collective impact on disease dynamics by capturing emergent behaviours such as vaccine hesitancy clustering, echo chambers, and behavioural resistance.

This study makes a novel theoretical contribution to the interdisciplinary domain of computational epidemiology, social simulation, and behavioural modelling by proposing a modular agent-based framework that explicitly integrates epidemiological, informational, cognitive, and policy-driven dimensions of infectious disease dynamics. Unlike empirical simulation studies that focus on retrospective case analysis or predictive forecasting, this study provides a generalized conceptual architecture intended to serve as a foundational model for future implementations and scenario testing.

In this paper, Section 2 (Current Research Analysis) provides a comprehensive review of recent agent-based modelling studies in the context of infectious disease simulation, emphasizing advances and limitations in modelling behavioural responses and misinformation dynamics. Section 3 (Methodology) details the structure and logic of the proposed modular framework, including its epidemiological, behavioural, informational, and logistic subsystems. This section also presents the modelling assumptions and key design principles. Section 4 (Case Study) applies the model to simulate a COVID-like outbreak under varying behavioural and informational conditions, highlighting the effects of vaccine hesitancy and corrective interventions. Section 5 (Discussion) interprets the results, situates the framework within the broader literature, and identifies implications for pandemic preparedness and communication strategy. Finally, the Conclusions summarize the theoretical and practical contributions of the model and outline directions for future research.

The current research is part of a comprehensive information system for assessing the impact of emergencies on the spread of infectious diseases described in [14].

2. Current Research Analysis

In recent years, agent-based modelling has become a prominent tool to simulate the spread of infectious diseases, particularly during the COVID-19 pandemic. Unlike traditional compartmental models, agent-based models enable the representation of individual-level behaviours, heterogeneity in decision-making, and complex interaction networks, features essential for capturing

ISSN 1814-4225 (print)
ISSN 2663-2012 (online)

disease transmission dynamics in socially and behaviorally diverse populations. The COVID-19 crisis has prompted a surge of research in this domain, resulting in a diverse body of work exploring the effects of NPIs, vaccine uptake, misinformation, social influence, and policy strategies through agent-based modelling frameworks. These models have proven especially valuable for evaluating scenario-based interventions and understanding emergent outcomes arising from behavioural feedback loops and unequal access to health resources. Moreover, the flexibility of agent-based approaches has allowed researchers to incorporate real-world data, simulate region-specific conditions, and test the robustness of policy decisions under uncertainty. This section critically reviews representative studies that employed agent-based approaches to model COVID-19 dynamics. The objective is to identify key modelling choices, thematic contributions, methodological innovations and current gaps that motivate the development of the theoretical framework presented in this paper.

In the study [15], we present COVSIM, a stochastic agent-based simulation model developed to analyze the spread of COVID-19 in North Carolina with high demographic and geographic resolution. The model simulates over 1 million agents representative of the state's 10.5 million population, incorporating detailed attributes such as age, race/ethnicity, high-risk medical status, and geographic distribution by census tract. COVSIM employs a time-varying interaction network structure, integrating household, peer group, and community layers to capture daily contact dynamics. The force of infection model drives disease transmission based on these interactions, with behaviour-modifying factors such as masking, vaccination, mobility and quarantine policies. The model includes adaptive components such as emerging variants, waning immunity, and case importation. Through multiple scenario analyses, including varying vaccine uptake and efficacy, NPI strategies, and equity-focused vaccination policies, the model was used to inform public health decisions at local and state levels, highlighting disparities in outcomes among historically marginalized populations and emphasizing the interdependence of subpopulations in shaping overall disease dynamics.

The study [16] presents a dynamic agent-based model was developed to simulate the COVID-19 epidemic in Agadir, Morocco, integrating a social network-based contact structure with detailed disease progression. The model extends the classical SEIR framework to a high-resolution state-transition structure, capturing heterogeneity in disease severity and healthcare resource use (normal beds, intensive care units (ICU), ventilators). The agents are embedded in small-world networks with Poisson-distributed degrees to simulate realistic contact patterns within and between communities. The model allows the exploration of interventions through variations in social connectivity, proportion of external contact, and mask-wearing probability. The proposed NetLogo model simulates daily dynamics and enables scenario comparisons. Results show that vaccination alone yielded high infection rates and ICU demand, whereas combining vaccination with moderate mask usage significantly flattens infection curves and reduces hospital burden.

The study by Ebrahimi et al. [17] developed an agent-based model for simulating COVID-19 transmission in closed indoor environments, calibrated using data from Calabria, Italy. The model incorporates direct, indirect (surface), and external infection pathways and is structured around a SEIRQD framework (Susceptible, Exposed, Infectious, Recovered, Quarantined, Deceased). Agent states include key behavioural and epidemiological variables, such as movement probability, vaccination status, and asymptomatic carriage. The simulation environment consisted of spatially distributed agents on a 36×36 meter grid, where each cell carried a virus concentration value. The model conducts a high-throughput sensitivity analysis over 4,374 parameter combinations (with 87,480 total runs), identifying transmission distance and agent movement as the most influential factors affecting total infections, peak size, and timing. The model was implemented in NetLogo and validated using RMSE, MAPE, and Chi-square metrics.

Erik Cuevas [18] proposed a simplified agent-based model for evaluating the transmission risk of COVID-19 within indoor facilities. Agents represent susceptible and infected individuals with unique mobility and infection probabilities, thereby simulating heterogeneity in compliance and health status. The model operates in a 2D continuous space where infection spreads via proximity-based rules, combining local and long-distance movements governed by a probability α. Infection occurs probabilistically if a susceptible agent is within an infected agent's defined radius. Key experiments were conducted to assess the impact of facility occupancy limits, population-level adherence to preventive behaviours (e.g., masking), and mobility restrictions. Results show that transmission risk increases sharply with occupancy above 300, preventive behaviour reduces risk significantly when adopted by 60%+ agents, and mobility restrictions delay or reduce outbreak severity. The model is computationally simple but capable of producing interpretable outputs relevant to localized intervention design.

The study [19] proposed a large-scale behavioural agent-based model built on SydneyGMA, a high-fidelity travel/activity simulator, to assess the effectiveness of various COVID-19 control strategies in Sydney's Greater Metropolitan Area. The model simulates daily activities, travel behaviours, and inter-agent contacts among 5.8 million synthetic individuals using TASHA (Travel/Activity Scheduler for Household Agents), linked with a disease spread simulator. The transmission

model includes detailed health states (susceptible, exposed, infectious, quarantined, recovered, deceased) and accounts for within-household and activity-based interactions. The authors introduce a structured calibration methodology using Response Surface Methodology and Central Composite Design to estimate interdependent parameters such as contact rates, infection probabilities, and incubation period. Sensitivity and scenario analyses were conducted to assess the impact of social distancing, travel load, facemask usage, and timing of interventions. The model's realism is enhanced by integrating actual travel demand patterns and public transport usage from Sydney, allowing for a robust evaluation of intervention strategies and interaction effects.

In the study [20], a behavioural agent-based model was introduced to simulate COVID-19 transmission and adaptive self-isolation behaviour in the United Kingdom. The model combines a demographic module (generating a synthetic UK population) with a 360-day pandemic simulation. Agents interact via dynamic social networks and attend spatially distributed venues, with viral transmission occurring through household and social contacts. A key innovation is a behavioural module that endogenously determines agents' self-isolation and testing decisions based on risk perception, social norms, public information, and household support networks. Subjective probabilities of infection, hospitalization, and death are formed through Bayesian-like updates using public data and personal network experiences. Sensitivity analysis identifies the most influential parameters affecting social behaviour, including responsiveness to local infection prevalence, income-constrained ability to isolate, and social influence. The resulting infection network exhibits a scale-free structure, with self-isolation behaviour significantly altering the transmission dynamics and mobility patterns.

In the study [21], a hybrid agent-based SEIR modeling framework was introduced to simulate COVID-19 transmission dynamics on a real construction site. Implemented in AnyLogic, the model integrates a modified SEIR structure with individual agent behaviours based on empirical survey data (n=175) and simulates interactions in a spatially accurate environment using a social force model. Key safety control measures, such as face covering, vaccination, ventilation, social distancing, and isolation, were incorporated at varying compliance levels to form 108 simulation scenarios. Each agent transitions through SEIR states with probabilities modulated by personal attributes (e.g., age, vaccination status), environmental exposure, and contact patterns. The simulation outputs include the hourly infection states, contact duration, and message-passing dynamics to assess the risk. Results reveal that full compliance with all safety control measures delayed infection onset and significantly reduced peak infection (by up to 75%). In contrast, partial compliance without isolation or ventilation still mitigates spread.

A previous study [22] presented a spatially explicit agent-based model developed in the GAMA platform to simulate the spatiotemporal spread of COVID-19 in a Polish district near Warsaw. The model incorporates demographic, mobility, and epidemiological data using a generalized SMEIRPD framework. Agents represent individuals with detailed routines and movement patterns based on day type (work vs. non-work), travel mode, and location type (e.g., home, work, shops). Infection probability was dynamically computed based on interpersonal distance, masking behaviour, atmospheric conditions (temperature, humidity), and restriction levels parameterized using the COVID-19 Stringency Index. The simulation evaluates three restriction scenarios: baseline (Poland), liberal (France), and unrestricted (Belarus), with validation against real incidence data. Results show significant variation in infection peaks and hospital overload risks depending on restriction severity and highlight the role of spatial structure and social mobility in epidemic trajectories.

The study by Bhattacharya et al. [23] presented a large-scale AI-driven agent-based modelling framework (EpiHiper) to evaluate the impact of vaccine acceptance on COVID-19 spread across the United States. The model uses a detailed synthetic population and dynamic contact network spanning all 50 states and Washington, D.C., comprising 288 million agents and over 12.5 billion daily interactions. Vaccination dynamics incorporate production schedules, hesitancy rates (sourced from Facebook surveys), prioritization strategies, and two distinct rollout tempos (accelerated and accelerated-decelerated). The simulation environment was powered by high-performance computing across dual clusters (Bridges2 and Rivanna), enabling over 6,000 simulation runs. This study shows that slow vaccination due to hesitancy significantly reduces averted cases and deaths, even if final coverage remains the same. The model further reveals that increasing vaccine acceptance by 10% can prevent up to 200,000 more infections nationwide. The framework captures spatiotemporal heterogeneity and supports multi-level policy evaluation under realistic demand constraints.

In the study [24], a spatially resolved agent-based model was proposed to simulate COVID-19 spread and vaccination strategies in Quezon City, Philippines. The model builds on the Age-Stratified Quarantine-Modified SEIR with nonlinear incidence rates (ASQ-SEIR-NLIR), incorporating age-stratified infection risks, behavioural (mask-wearing, distancing), and physiological (low immunity) modifiers, and GIS-based spatial distribution using Mesa and MesaGeo in Python. The model includes stochastic agent transitions between SEIRDV states and models' quarantine success (Q), age-dependent

ISSN 1814-4225 (print)
ISSN 2663-2012 (online)

susceptibility (U), and nonlinear exposure dampening through α and ε parameters. The simulation compares four vaccination scenarios using coupled multi-objective linear programming optimization for equitable distribution based on prioritization criteria (e.g., mobile workers, elderly, low-income groups). Results show that prioritizing mobile workers reduces infections most (−4.34%), while prioritizing low-income groups reduces deaths most (−1.93%). The model was calibrated using data from the Philippine Department of Health and validated against a 60-day incidence.

The reviewed studies demonstrate the versatility and sophistication of agent-based models in simulating COVID-19 dynamics across various spatial, behavior-albehavioural, and policy contexts. These models incorporate diverse methodological innovations, including social networks, high-resolution geospatial data, behavioural adaptation, and vaccination logistics. While each study emphasizes different aspects, such as mobility, vaccine hesitancy, or spatial heterogeneity, they collectively highlight the critical importance of integrating epidemiological and socio-behavioural factors. The analysis provides a strong empirical and conceptual foundation for the theoretical framework proposed in this study, which seeks to unify epidemiological modelling with misinformation dynamics, belief-driven vaccine uptake, and policy interventions.

Table 1

Current state of agent-based infectious disease simulation

Paper	Task	Data	Findings
Rosenstrom et al. [15]	Modeling COVID-19 transmission dynamics under various vaccination, masking, and policy scenarios with demographic heterogeneity	Epidemiological data (hospitalizations, deaths), census data (age, race/ethnicity), vaccination uptake, masking behaviour (survey), mobility (SafeGraph), and public health policy timelines.	The time-varying interaction network captures detailed contact dynamics. The extended SEIR structure facilitates variant-specific progression and reinfection. The model demonstrates strong sensitivity to vaccine uptake timing and NPI adherence. The stratified outputs reveal significant disparities due to demographic heterogeneity.
Nemiche et al. [16]	Simulating COVID-19 spread under vaccination and mask scenarios using a social network-based agent-based model	Population structure (Agadir), age-stratified severity/fatality rates, hospital capacity assumptions	Fine-grained SEIR model with detailed symptom states and hospital routing. The social network structure affects the spread of information. Vaccination alone is insufficient; adding 50% masking reduces infections by ~80% and ICU demand by >70%.
Ebrahimi et al. [17]	Simulating COVID-19 transmission in closed indoor settings using multi-source infection mechanisms and parameter sensitivity	Epidemiological data from Calabria, Italy (incidence, test counts); agent parameters from prior literature	SEIRQD-based agent-based model with direct, indirect, and external infection routes. Sensitivity analysis of 4374 scenarios identified transmission distance, asymptomatic rate, and mobility as the most influential parameters. The surface transmission is minor (<1%).
Cuevas [18]	Assessing COVID-19 transmission risk in indoor facilities with varying behavioral and spatial configurations	Synthetic population, spatial layout assumptions, WHO infection radius, and assumed infection/mobility probabilities	2D spatial agent-based model with probabilistic infection/movement rules. The transmission risk increases nonlinearly with density and mobility. A 60% preventive compliance or full mobility restriction significantly reduces the outbreak speed and size.
Najmi et al. [19]	Evaluate COVID-19 control strategies (social distance, travel limits, facemasks, quarantine timing)	Synthetic population (Sydney), activity-travel patterns (TASHA), COVID-19 incidence, PT usage, policy dates	Large-scale agent-based model. Social distancing compliance of 85.9% was needed to suppress the spread of the disease. Early lockdowns reduce cases by up to 96%. Facemask use >80% compensates for moderate social distancing in reopening scenarios.
Gostoli and Silverman [20]	Model feedback between COVID-19 dynamics and adaptive isolation/testing behaviour	UK census, mobility reports, and empirical hospitalization/death rates	Agent-based model with endogenous isolation/testing via social-cognitive model. The key drivers of isolation are local infection rates, income levels, and network norms. Results produce scale-free infection networks and confirm strong behavioural feedback effects.

Paper	Task	Data	Findings
Qiao et al. [21]	Assess the effectiveness of COVID-19 spread and safety control measures in a real construction site	Survey data (n=175), work schedules, site layout, and literature-based SEIR parameters	Agent-based SEIR model with mobility-based safety control measures. The 108 SCM scenarios show that full compliance reduces peak infections by 75%, with isolation and vaccination most effective. Social distancing was less impactful due to canteen clustering.
Olszewski et al. [22]	Simulating spatiotemporal COVID-19 spread under varying restriction levels	GIS spatial data, demographic (age, mobility), local COVID-19 incidence, atmospheric conditions, policy stringency index	SMEIRPD agent-based model with 15-min agent resolution. Infection risk is influenced by distance, masking, mobility, and weather. Unrestricted scenario causes 10× higher peak and ICU overflow. Spatial heterogeneity shapes outbreak patterns.
Bhattacharya et al. [23]	Modeling of nationwide COVID-19 dynamics under different vaccine acceptance and rollout strategies	Synthetic population (288M), Facebook vaccine hesitancy surveys, CDC parameters, NHTS/ATUS/MTUS, NYT incidence data	US-scale SEIR agent-based model with dynamic contact networks. Vaccine hesitancy reduces averted infections from 6.7M to 4.5M. Increasing the acceptance by 10% adds 200 K averted cases. State outcomes vary according to social vulnerability and population size.
Bongolan et al. [24]	Simulating and optimizing vaccination strategies in Quezon City, Philippines	Quezon City population projections, DOH incidence/deaths, behavioural rates (masking, distancing), income by district	GIS-based agent-based model with SEIRDV structure and nonlinear incidence. Prioritizing mobile workers reduces infections (−4.34%), and low-income prioritization reduces deaths (−1.93%). Stochastic runs with multi-objective linear programming optimize district-wise vaccine allocation.

3. Methodology

The agent-based model developed in this study adopts a modular, multi-layered structure that integrates behavioural, informational, and epidemiological subsystems to simulate the spread and control of an infectious disease (with an example of COVID-19) in a heterogeneous population. The model architecture reflects the complex interdependencies between individual decision-making, social influence, information environments, and health system dynamics.

The model consists of four tightly coupled subsystems:

1. The epidemiological subsystem governs transitions between health states (Susceptible, Exposed, Infectious, Recovered, Deceased, Vaccinated) using a modified SEIRDV structure. This compartmental framework is sensitive to agent-level immunity, which evolves dynamically through vaccination.

2. The behavioural subsystem captures individual heterogeneity in vaccination decisions. Each agent maintains internal vaccination willingness scores influenced by cognitive and social factors. These include exposure to misinformation, susceptibility to peer influence, and sociological clustering derived from empirical attitudinal profiles.

3. The misinformation propagation subsystem models the diffusion of misinformation through the agent network. Belief dynamics evolve via peer interactions and exogenous shocks, reinforcing or weakening vaccine hesitancy.

4. The vaccination logistics subsystem constrains decision outcomes through structural factors, such as dose availability, prioritization policies, and time delays. The method encodes the gap between willingness and access and allows the simulation of targeted or randomized intervention strategies.

The overall model is designed to simulate emergent behaviour at the population level as a function of local interactions between agents and external constraints. Figure 1 illustrates the interaction flow across subsystems: beliefs and norms shape willingness; willingness and supply govern vaccination; immunity affects health state; and health feedback modifies beliefs and behaviours.

The model starts from the top with the Sociological Cluster (C_i), which influences Misinformation Exposure and Social Influence. These two factors contribute to the computation of Vaccination Willingness (VW_i). Willingness, along with Vaccine Supply and Policy, determines the Vaccination Process. Vaccination then updates the agent's Immunity Level (ε_i), directly affecting their Health State (SEIRDV). Finally, the agent's health status loops back and modifies social and informational dynamics.

ISSN 1814-4225 (print)
ISSN 2663-2012 (online)

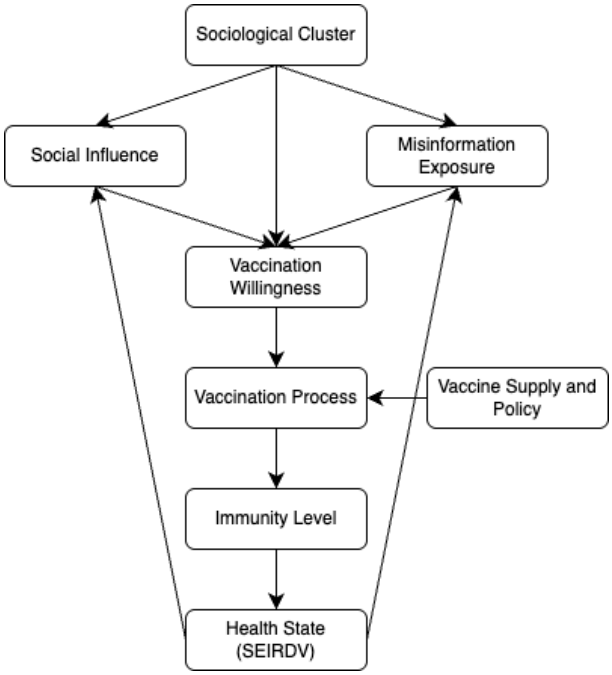

Figure 1. The model's architecture

This modular decomposition allows for high interpretability and targeted experimentation while capturing the nonlinear feedback loops that characterize real-world epidemic dynamics in socially complex settings.

3.1. The epidemiological Subsystem

The foundational layer of the agent-based system models the spread of COVID-19 using a discrete-time, stochastic extension of the classic SEIR framework. The model incorporates additional compartments for vaccinated and deceased agents to capture the complexity of real-world epidemic processes and intervention strategies, resulting in a six-state health transition model: SEIRDV. Each state transition is governed by a set of biologically informed probabilistic rules and occurs on a per-agent basis at each simulation time step.

Each agent $i \in \{1, 2, \ldots, N\}$, where N denotes the total number of agents in the population, is assigned a health state $X_i(t) \in \{S, E, I, R, V, D\}$ at each discrete time point t, as detailed below:

1. Susceptible (S): The agent is healthy but lacks immunity to SARS-CoV-2 and is vulnerable to infection upon contact with infectious individuals.

2. Exposed (E): The agent was infected but not yet infectious. This state represents the incubation or latent period between infection and the onset of contagiousness.

3. Infectious (I): The agent can transmit the virus to others via contact. Epidemiological parameters govern the infectious period and may terminate during recovery or death.

4. Recovered (R): The agent has cleared the infection and is assumed to have acquired immunity during the simulation. In the current iteration, reinfection is not modeled.

5. Vaccinated (V): The agent has received a COVID-19 vaccine and is assumed to have partial or full immunity. The level of protection is determined by the vaccine efficacy parameter \epsilon.

6. Deceased (D): The agent has died due to infection and has been removed from the simulation's dynamic processes.

The transitions between these compartments follow stochastic rules grounded in epidemiological theory and empirical data, as described below. As a conceptual foundation, the model adopts the structure of a compartmental SEIRDV system defined by the differential equations (1).

$$\begin{cases} \frac{dS}{dt} = -\beta\frac{SI}{N} - \lambda S \\ \frac{dE}{dt} = \beta\frac{SI}{N} - \sigma E \\ \frac{dI}{dt} = \sigma E - \gamma I - \mu I \\ \frac{dR}{dt} = \gamma I \\ \frac{dV}{dt} = \lambda S \\ \frac{dD}{dt} = \mu I \end{cases} \quad (1)$$

where β is the transmission rate per susceptible-infectious interaction, λ is the vaccination rate, σ is the transition rate from exposure to infection (i.e., inverse of incubation period), γ is the recovery rate, and μ is the disease-induced mortality rate.

This deterministic model serves as a reference to justify the structure of the agent-based implementation, which introduces heterogeneity, distinct stochastic transitions, and network-based interactions. The transitions between states are presented in Figure 2.

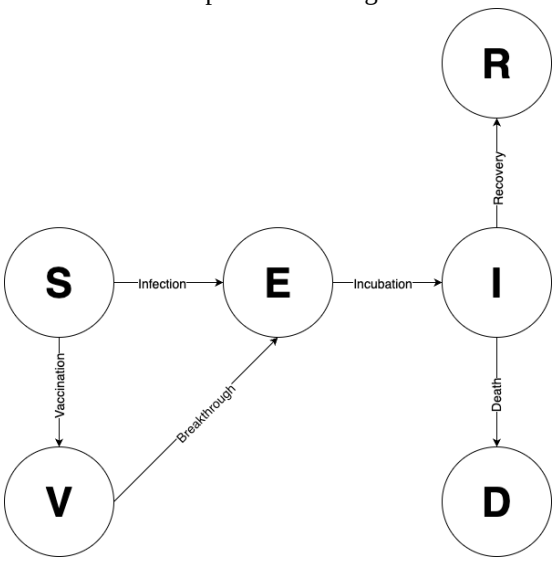

Figure 2. Transition between agent's states

In an agent-based context, time progresses in separate intervals $t \in \mathbb{N}_0$, and transitions between states occur probabilistically based on local interactions and individual-level attributes. Here, X_i(t) denotes the health state of agent i at time t. The model assumes a fixed contact network G = (V, E), where each node represents an agent, and edges represent potential for interaction and disease transmission.

The transition probabilities for each possible change in the health state is defined below.

A susceptible agent i, in contact with a set of neighbours $N_i \subseteq V$, becomes exposed with probability determined by the infectiousness of those neighbours. The probability of avoiding infection from a single infectious contact $j \in N_i$ is $1 - \beta_{ij}$, where $\beta_{ij} \in [0,1]$ is the per-contact transmission probability. Assuming independence across contacts, the overall probability of remaining uninfected is the product of all such escape probabilities as follows:

$$P(S_i(t) \to E_i(t+1)) = 1 - \prod_{j \in N_i} \left(1 - \beta_{ij} \cdot 1_{\{X_j(t)=I\}}\right) \quad (2)$$

This formulation allows for heterogeneity in contact strength and models local spread based on the agent's immediate neighbourhood.

Agents transition from the exposed to infectious state with a constant probability σ, reflecting the average duration of the incubation period as follows:

$$P(E_i(t) \to I_i(t+1)) = \sigma \quad (3)$$

In biological terms, this corresponds to the latent period during which the virus replicates but is not yet transmissible.

Infectious agents have two mutually exclusive outcomes: recovery or death. The model applies Bernoulli trials using the probabilities γ and μ, respectively:

$$P(I_i(t) \to R_i(t+1)) = \gamma \quad (4)$$
$$P(I_i(t) \to D_i(t+1)) = \mu \quad (5)$$

To ensure a valid probability distribution, it is required that $\gamma + \mu \leq 1$; any remaining probability mass accounts for the possibility that the agent remains infectious at the next time step.

Vaccination occurs stochastically based on both external access and internal willingness, which are formally integrated in later iterations. In the present study, vaccination is represented as a probabilistic event with rate $\lambda_i(t) \in [0,1]$, which may vary across agents and time:

$$P(S_i(t) \to V_i(t+1)) = \lambda_i(t) \quad (6)$$

This transition model of individual participation in a vaccination campaign may be conditioned on policy interventions, vaccine supply, or sociological traits.

Vaccinated individuals retain some susceptibility to infection, depending on the vaccine efficacy $\varepsilon \in [0,1]$. The probability of infection by a vaccinated agent is reduced by a factor $(1 - \varepsilon)$, applied to the same exposure dynamics as that of susceptible individuals:

$$P(V_i(t) \to E_i(t+1)) = (1 - \varepsilon) \cdot P(S_i(t) \to E_i(t+1)) \quad (7)$$

This formulation supports realistic modelling of breakthrough infections under varying vaccine effectiveness, including strain-dependent and waning immunity effects in future versions.

The agent-based epidemiological model relies on a set of key parameters that govern the rates of disease progression, transmission, mortality, vaccination, and breakthrough infections. These parameters can be fixed across the agent population or drawn from distributions to reflect inter-individual heterogeneity. Table 2 summarizes the primary epidemiological parameters used in this iteration, along with interpretations and typical values reported in the literature.

The transmission probability β_{ij} can be modelled as heterogeneous across pairs of agents, allowing for individual variations in infectiousness (e.g., superspreaders) and environmental contexts (e.g., indoor vs outdoor settings). The recovery and mortality rates are assumed to be independent but may be conditioned on agent-level health characteristics (e.g., age, chronic illness). The vaccination probability $\lambda_i(t)$ is designed to be dynamic and behaviorally informed. It serves as a placeholder for pending integration with the behavioural subsystem. The vaccine efficacy ε in this model reduces only the probability of infection; extension for other diseases may allow it to reduce infectiousness, symptom severity, or mortality. These parameters can be specified globally or drawn from empirical distributions to introduce demographic and behavioural heterogeneity.

The current iteration of the model adopts a set of simplifying the assumptions intended to isolate and accurately represent the core epidemiological mechanisms of SARS-CoV-2 transmission and progression. These assumptions are articulated explicitly below to clarify the scope of the subsystem and highlight areas for potential refinement in subsequent development stages:

– Fixed Immunity Duration. Agents who recover from infection or receive a vaccine are assumed to have complete immunity for the remainder of the simulation. This eliminates the possibility of reinfection or waning vaccine protection. While this assumption simplifies the model dynamics, it can be relaxed in future iterations by introducing immunity duration parameters or time-dependent efficacy decay;

ISSN 1814-4225 (print)
ISSN 2663-2012 (online)

Table 2

Epidemiological parameters

Parameter	Description	Interpretation	Typical values	Source
β_{ij}	Contact-specific transmission probability	Probability of agent i becoming infected upon contact with infectious agent j	0.01 – 0.25	Based on reproduction number $R_0 \approx 24$ and contact network density [25]
σ	Incubation rate	Probability of progressing from exposure to infectious state per time step	0.2 (1/5 days)	Reflects the 5-day average incubation [26]
γ	Recovery rate	Probability of recovery of an infectious individual in a given time step	0.1 (1/10 days)	The average infectious period of ~10 days [26]
μ	Mortality rate	Probability of death from infection per time step	0.001 – 0.01	Depends on age, comorbidities, and healthcare access
$\lambda_i(t)$	Vaccination probability of agent i	Probability of a susceptible agent being vaccinated at time t, conditional on availability and willingness	Varies by policy, supply, and behaviour	The intervention modules of the model
ε	Vaccine efficacy	The proportional reduction in infection risk due to vaccination	0.5 – 0.95	Depends on the vaccine type and strain [27]

– Homogeneous Disease Progression. All agents exhibit identical progression rates between health states (i.e., \sigma, \gamma, \mu are fixed). This reflects an average epidemiological profile and does not account for demographic or clinical heterogeneity. Future model extensions may stratify agents by risk factors (e.g., age, comorbidities) using parameter values drawn from stratified distributions;

– Static Contact Network. The social network G = (V, E), which governs exposure opportunities, is assumed to be fixed over time. This implies that agents interact with the same set of contacts at each time step. Although static networks are computationally tractable and widely used, real-world contact patterns exhibit temporal variation due to movement restrictions, behaviour changes, and seasonality. Dynamic or activity-based networks can be implemented in later iterations;

– No Behavioral Response to Infection. In this initial epidemiological module, agents do not alter their behaviour upon infection or based on perceived risk (e.g., reducing contacts, isolating, or seeking testing). Incorporating adaptive behaviour in response to personal- or community-level infection is addressed in the behavioural subsystem;

– Instantaneous Transitions. State transitions are evaluated and executed synchronously at each time step, assuming no delay between the decision and outcome. For example, vaccine-induced immunity is granted immediately after vaccination. Versions for other diseases may incorporate delay states or lagged effects to better mimic real-life biological processes;

– Uniform Vaccine Efficacy. All vaccinated agents will receive the same level of protection, regardless of age, vaccine brand, or number of doses. This assumption facilitates simplicity and interpretability but can be relaxed to model mixed vaccine regimes and differential effects (e.g., mRNA vs vector vaccines).

These assumptions enable computational efficiency and conceptual clarity during the model's foundational phase. However, they are not intended to remain fixed in the final implementation. Rather, they provide a controlled baseline for systematically testing the effects of increasingly complex behavioural and structural mechanisms introduced in later iterations.

3.2. The Behavioural Subsystem

To simulate individual-level variation in cognitive, social, and behavioural responses during a pandemic, each agent in the model is equipped with a rich set of internal attributes. These attributes determine how an agent perceives risk, processes information, and makes decisions regarding vaccination and public health recommendations. The architecture supports the emergence of heterogeneous behavioural patterns within a shared epidemiological landscape.

Each agent $i \in \{1, 2, \ldots, N\}$ is represented as a tuple of cognitive, social, and epidemiological states. In addition to the health status variables described in the epi-

demiological subsystem. The dynamic attributes assigned to the agents are summarized in Table 3.

This attribute structure provides a formal schema for representing the socially embedded cognition of individuals during an infectious disease outbreak. The proposed model also supports modular integration with other components of the agent-based model.

The variables $M_i(t)$, $SI_i(t)$ and $VW_i(t)$ evolve over time in response to social signals, media exposure, and observed behaviours. These dynamics allow the model to simulate agents who adapt their beliefs and behaviours based on personal and environmental factors.

The sociological cluster C_i is a categorical variable that governs the start of behavioural parameters and their sensitivity to inputs. For instance, conformists may begin with moderate vaccination willingness but are highly sensitive to $SI_i(t)$, whereas skeptics have a low initial willingness and are immune to peer influence.

The decision threshold θ_i introduces heterogeneity in decision-making styles. Even if two agents have identical vaccination willingness $VW_i(t)$, one may act while the other delays, depending on this internal cutoff. Thresholds can be initialized randomly, drawn from a specified distribution, or defined by demographic variables (e.g., age, education level).

The social network N_i defines the agent's sphere of influence and is used to model both disease transmission and belief propagation. Edges (i, j) may carry weights w_{ij} representing the strength of influence, such that misinformation or behavioural norms from close peers are more impactful than those from weak ties.

Agents are categorized into sociological clusters $C_i \in \{1, 2, 3, 4\}$, each representing a distinct behavioural archetype based on empirical studies of vaccine-related attitudes. These archetypes reflect opinions on vaccination and deeper orientations toward authority, peer influence, and medical trust. The assignment is probabilistic based on the observed population distributions [28]. The sociological clusters are presented in Table 4.

Table 3

Agent's dynamic attributes

Parameter	Description	Type	Description
C_i	Social cluster	Categorial	Attitudinal classification based on vaccine beliefs (supporter, loyalist, conformist, skeptic) shapes baseline dispositions.
$M_i(t)$	Misinformation exposure	Continuous [0,1]	Dynamic belief score representing the agent's level of exposure to or acceptance of health-related misinformation
$SI_i(t)$	Social influence score	Continuous [0,1]	The degree to which an agent is influenced by the behaviour and expectations of social contacts
$VW_i(t)$	Vaccination willingness	Continuous [0,1]	The time-varying probability that the agent will accept vaccination is determined by $M_i(t)$, $SI_i(t)$, and sociological priors.
θ_i	Decision threshold	Continuous [0,1]	Individual-specific internal cutoff value determining when willingness leads to action (i.e., vaccination)
N_i	Network neighbourhood	Set	The subset of the population with whom the agent interacts governs information and disease exposure
w_{ij}	Edge weights	Continuous [0,1]	The influence strength of agent j on agent i, defining heterogeneous social ties
$\phi(C_i)$	Cluster bias function	Scalar	Encodes predisposition toward vaccination based on sociological type (e.g., high for supporters, low for skeptics)

Table 4

Social clusters

Cluster	Label	Description	Behaviour Profile
1	Supporters	Strongly pro-vaccine, they perceive vaccination as civic duty	High baseline VW_i, low M_i, low θ_i
2	Loyalists	Support vaccination but resist mandates or politization	Moderate VW_i, moderate SI_i, and low-moderate M_i
3	Conformists	Indifferent or ambivalent; follow peers and institutions	High SI_i, low personal initiative, and variable VW_i
4	Skeptics	Distrust of vaccination, institutions, and official narratives	High M_i, low VW_i, high θ_i

ISSN 1814-4225 (print)
ISSN 2663-2012 (online)

These clusters determine the agent's initial cognitive profile and act as moderators in updated equations, shaping their sensitivity to peer behaviour and misinformation. For example, skeptics may exhibit low social learning rates and higher resistance to corrective information.

Misinformation is a dynamically evolving belief signal that influences risk perception and health behaviour. The score $M_i(t) \in [0,1]$ represents the degree to which an agent is influenced by false or misleading health information at time t. This can include vaccine myths, conspiracies, and pseudoscientific narratives. This function allows the model to simulate local reinforcement (echo chambers) and global shocks during information exposure.

The misinformation rule is defined as follows:

$$M_i(t+1) = (1-\delta)M_i(t) + \frac{\eta}{|N_i|}\sum j \in N_i w_{ij} M_j(t) + \xi_i(t) \quad (8)$$

where $\delta \in [0, 1]$ is the natural decay rate (e.g., through corrective experiences or fact-checking), η is social susceptibility coefficient, modulated by sociological cluster, w_{ij} is the edge weight from agent j to i, reflecting trust or influence strength, $\xi_i(t)$ is exogenous misinformation exposure, such as social media content or foreign propaganda, which can be modelled stochastically or via scenario-based events.

Agents in cluster 4 (skeptics) may have a reduced δ, leading to persistent misinformation beliefs. Mass misinformation events (e.g., viral disinformation campaigns) may be encoded as follows for relevant subsets of the population:

$$\xi_i(t) \sim N(\mu, \sigma^2). \quad (9)$$

The social influence score $SI_i(t) \in [0, 1]$ captures the perceived normative pressure to adopt a behaviour (e.g., get vaccinated). It is shaped by two components:

1. Descriptive norms are the prevalence of behaviour among an agent's social contacts.

2. Injunctive norms are perceived expectations about what one "should" do

The rule is as follows:

$$SI_i(t+1) = \rho_d \cdot \frac{1}{|N_i|}\sum j \in N_i w_{ij} \cdot v_j(t) + \rho_i \cdot \psi_i(t) + (1-\rho_d-\rho_i)\cdot SI_i(t) \quad (10)$$

where ρ_d, ρ_i are weighting factors for descriptive and injunctive norms, respectively ($\rho_d + \rho_i \leq 1$); $v_j(t)$ is the vaccination status of agent j, defined as 1 if agent j is vaccinated at time t, 0 otherwise; w_{ij} is the influence weight of agent j on agent I, representing trust or social connectivity; $\psi_i(t)$ represents external injunctive norms, such as public health messaging, mandates or advocacy. The final term, $(1 - \rho_d - \rho_i)SI_i(t)$ represents norm retention, ensuring continuity in the agent's perception of social norms over time.

The sociological cluster of each agent modulates sensitivity to social influence. Conformists (C_3) have higher ρ_d, making them more responsive to peer behaviour. Skeptics (C_4) have lower w_{ij} values (especially for official sources), reducing their susceptibility to normative pressure. Loyalists (C_2) may respond negatively to strong injunctive norms ($\psi_i(t)$), leading to an inverse effect in which enforcement reduces $SI_i(t)$.

This formulation allows the model to capture both peer-driven vaccine uptake and top-down policy influence, as well as resistance effects in skeptical subpopulations.

Vaccination willingness is a composite cognitive state reflecting the agent's internal decision readiness. It is calculated as a weighted sum of misinformation resistance, social pressure, and sociological bias:

$$VW_i(t) = \alpha_1 \cdot (1 - M_i(t)) + \alpha_2 \cdot SI_i(t) + \alpha_3 \cdot \phi(C_i) \quad (11)$$

where α_1, α_2, $\alpha_3 \in [0, 1]$ are weighted coefficients (calibrated by context or learning); $\phi(C_i)$ is cluster-based baseline disposition.

This model supports both linear and nonlinear transformations. To enable the modeling of hesitation, social tipping points or saturation effects, the simulation of threshold crossing and behavioral inertia can be presented as follows:

$$VW_i(t) = \frac{1}{1 + \exp\left(-k\left(\alpha_1(1 - M_i(t)) + \alpha_2 SI_i(t) + \alpha_3 \phi(C_i) - \theta_i\right)\right)} \quad (12)$$

where θ_i is an individual-specific activation threshold; k is the steepness parameter, which controls the decision sensitivity.

At each time step, susceptible agents evaluate whether or not to receive a vaccine if available. The decision is modelled as a threshold function as follows:

$$X_i(t+1) = \begin{cases} V, \text{if } VW_i(t) \geq \theta_i \\ S, \text{otherwise} \end{cases} \quad (13)$$

This rule reflects bounded rationality. Agents act when their internal motivation exceeds a threshold of action. The threshold $\theta_I \in [0,1]$ may be fixed (e.g., cluster-based), drawn from a distribution or adapted over time (e.g., decision fatigue or information overload).

The vaccination function can be further refined by including supply constraints (via ARIMA model results), eligibility windows (age, risk factors) and wait times or logistic delays.

The behavioural subsystem transforms agents from static health entities into dynamic decision-makers capable of adapting to their social context and information landscape. These cognitive extensions enable the model to capture the emergence and persistence of vaccine hesitancy, clustered behavioural resistance and the influence of social dynamics on public health. When integrated with the health transition model, these behavioural outputs, particularly vaccination decisions, directly affect epidemic dynamics.

3.3. The Misinformation Propagation Subsystem

The misinformation propagation subsystem defines the mechanisms by which health-related misinformation, particularly regarding COVID-19 vaccines, propagates throughout the agent population. Each agent maintains a time-varying scalar variable $M_i(t) \in [0,1]$, representing their belief alignment with false or misleading information. The dynamics of this score are informed by peer-to-peer interactions within a social network, exogenous media input, and internal psychological parameters reflecting susceptibility and skepticism.

The misinformation subsystem plays a dual role. First, it operationalized the effect of exposure to low-quality or malicious information on individual cognitive states. Second, it enables the simulation of coordinated disinformation campaigns, echo chamber formation, and the efficacy of corrective communication strategies. This integration is essential for capturing the interplay between beliefs, behaviours, and health outcomes in the context of contemporary pandemics.

The central function of this subsystem is to determine the evolution of an agent's misinformation exposure score over time. The belief update function for agent i at time t is formalized as (8).

The first term of the equation, $(1 - \delta_i)M_i(t)$, represents the memory persistence or retention of the current misinformation state. The scalar parameter $\delta_i \in [0,1]$ denotes the decay rate of misinformation belief for agent i, capturing the agent's natural tendency to revise, discount, or forget misleading beliefs over time. A high value of δ_i implies rapid decay and more significant skepticism, while lower values reflect belief inertia or resistance to correction.

The second term encodes the social reinforcement of misinformation through interactions with neighboring agents in the contact network N_i. Each neighbour j contributes a portion of their misinformation score $M_j(t)$, which is scaled by the directed edge weight $w_{ij} \in [0,1]$, which quantifies the influence of agent j on agent i. The influence of neighbours is aggregated and normalized by the size of the neighbourhood $|N_i|$, ensuring that the magnitude of social exposure remains stable across agents with varying degrees.

The final term, $\xi_i(t)$, introduces external informational signals outside the agent's immediate social contacts. This signal may represent background media exposure, algorithmic content delivery, or intentional disinformation campaigns and is treated as an exogenous stochastic process. The distribution and structure of $\xi_i(t)$ may vary over time or among individuals.

Together, these components simulate a feedback system in which misinformation persists, spreads, and evolves based on endogenous social interactions and exogenous informational pressures.

To capture the heterogeneous psychological makeup of the population, both the decay rate δ_i and the social susceptibility parameter η_i are defined at the individual level. These parameters introduce variations in belief dynamics that reflect known correlates of misinformation susceptibility, such as education, trust in institutions, and prior political beliefs.

The parameter δ_i governs the rate at which agent i forgets or corrects misinformation. It modulates the weight of prior belief $M_i(t)$ in the update function. Conceptually, it represents cognitive flexibility or openness to correction. An agent with $\delta_I = 0.5$ retains only half of their previous misinformation score at each step, whereas an agent with $\delta = 0.05$ exhibits persistent beliefs. In the model, δ_i may be drawn from a cluster-dependent distribution, reflecting systematic differences across sociological groups. For instance, individuals classified as skeptics may receive lower values of δ_i, making their beliefs more resistant to decay, even under social pressure.

The susceptibility parameter η_i controls the agent's receptivity to social misinformation signals. It acts as a global scaling factor on the peer influence term in the update equation. A higher η_i implies that the agent is strongly shaped by the beliefs of others in the network, whereas a lower η_i indicates social immunity or selective processing. This variable allows the model to simulate socially contagious belief systems in behaviorally conformist populations or to evaluate information critically.

These parameters, δ_i and η_i, are not static but may themselves be functions of the agent's sociological cluster, media literacy, or exposure history, allowing for future extensions such as adaptive cognition or reinforcement learning.

Here, set N_i denotes the immediate social network neighbourhood of agent i. The influence of neighbours is not uniform but instead weighted by w_{ij}, which captures trust, communication frequency, or shared identity. The misinformation aggregation term,

ISSN 1814-4225 (print)
ISSN 2663-2012 (online)

$$\frac{1}{|N_i|}\sum j \in N_i w_{ij} M_j(t) \quad (13)$$

can be interpreted as a weighted average misinformation signal received by agent i at time t. This formulation enables the emergence of localized misinformation clusters or "hotspots" when networks are highly modular or homophilic.

In scenarios where w_{ij} is uniform across all edges, this reduces to a simple average. However, in more realistic networks (e.g., scale-free or small-world graphs), differential weighting leads to non-linear diffusion patterns and facilitates the formation of echo chambers.

The exogenous term $\xi_i(t)$ in the update rule captures non-network-based misinformation exposure. This category includes passive exposure to general misinformation circulating in mass media or social platforms and targeted exposure due to algorithmic personalization or intentional disinformation campaigns.

For general modelling, $\xi_i(t)$ can be drawn from a zero-mean noise distribution such as (9). Alternatively, for distinct misinformation events, $\xi_i(t)$ can be modeled as follows:

$$\xi_i(t) = \begin{cases} A, \text{if } t \in T_{event} \text{ and } i \in \Omega \\ 0, \text{otherwise} \end{cases} \quad (14)$$

where A is the intensity of the misinformation campaign, T_{event} is the set of time steps when the campaign is active, and $\Omega \subseteq \{1, \ldots, N\}$ is the target group (e.g., susceptible or undecided agents). This construct enables a realistic simulation of strategic disinformation interventions, such as those deployed by state actors during health crises.

To assess the structural dynamics of misinformation propagation, we define an echo chamber $EC_k \subseteq V$ as a connected subgraph in which misinformation is both high in intensity and homogeneously distributed. Formally, a subnetwork qualifies as an echo chamber if both conditions are satisfied:

$$\frac{1}{|EC_k|}\sum_{i \in EC_k} M_i(t) > \tau_{EC} \quad (15)$$

$$\forall i \in EC_k, \frac{|N_i \cap EC_k|}{|N_i|} > \gamma \quad (16)$$

The parameter τ_{EC} sets a belief threshold (e.g., 0.7), and γ controls internal connectivity (e.g., 0.8), requiring that most social ties remain within the chamber. These structures are prone to self-reinforcement because contradictory signals rarely disrupt internal consensus. The existence and persistence of echo chambers can be evaluated longitudinally to assess whether public health communication strategies can break epistemic bubbles.

Public health agencies often attempt to counteract misinformation through fact-checking, social inoculation, and influencer-driven campaigns. These interventions can be operationalized in two primary ways:

1. Increasing the decay rate $\delta_i(t)$ temporarily or permanently for affected agents simulates a heightened sensitivity to correction as follows:

$$\delta_i(t) = \delta_i + \Delta\delta \quad (17)$$

for $t \in T_{intervention}$, $i \in \Omega_{targeted}$.

2. Injecting anti-misinformation agents into the network (e.g., trusted experts, community leaders) with low misinformation scores and high influence weights w_{ij}. These agents act as corrective hubs, diffusing low-belief signals and disrupting echo chamber dynamics.

The effects of such strategies can be evaluated through simulation experiments, observing reductions in average misinformation scores, delays in belief saturation, or increases in vaccine willingness.

This subsystem models the formation and evolution of belief under uncertainty, embedding individual misinformation exposure within a social and informational ecosystem. The formal structure supports the fine-grained simulation of heterogeneous belief dynamics and social susceptibility, time-varying misinformation campaigns and public health interventions, and structural phenomena such as echo chambers, amplification, and resistance.

As a cognitive state, the misinformation score $M_i(t)$ is directly fed into behaviour (via vaccination willingness) and indirectly into epidemiological outcomes. Thus, the misinformation propagation subsystem forms a critical bridge between communication, cognition, and contagion, enabling a comprehensive exploration of the complexity of a pandemic.

3.4. The Vaccination Logistics and Policy Interventions Subsystem

This subsystem integrates logistical constraints, distribution strategies, and policy scenarios into the simulation of COVID-19 vaccination campaigns. The framework builds upon the cognitive and behavioural layers established in previous sections by conditioning vaccine access not only on willingness but also on supply, timing, prioritization, and public health interventions.

According to the previous subsystems, agents' decisions to receive vaccination were governed primarily by internal cognitive processes, including misinformation exposure, social influence, and sociological predisposition. However, vaccination behaviour in the real world is not determined solely by willingness. It is also a function of structural availability, policy-driven eligibility, and distribution capacity.

This subsystem describes mechanisms for representing vaccine supply dynamics, scheduling constraints, prioritization strategies, and policy interventions. This defines whether a willing agent can actually receive a vaccine at a given time and simulates how interventions such as mandates, targeted campaigns, and availability shocks influence uptake and epidemic trajectories.

Here, let $V_{available}(t)$ denote the number of vaccine doses available in the system at time step t. This value is exogenous and can be modelled using an empirical forecast, scenario-specific function, or historical rollout data.

Here, $E_i(t) \in \{0, 1\}$ be an indicator function specifying whether agent i is eligible to receive a vaccine at time t. A combination of system-wide policies and individual attributes, such as age, occupation, risk status, and prior infection history, may determine eligibility. The function can be defined as follows:

$$E_i(t) = \begin{cases} 1, \text{if } i \in P_t \text{ and } X_i(t) = S \\ 0, \text{otherwise} \end{cases} \quad (18)$$

where $P_t \subseteq \{1, .., N\}$ is the priority group eligible for vaccination at time t, and $X_i(t) = S$ ensures that the agent is susceptible and has not already been vaccinated or infected.

If both $E_i(t) = t$ and $VW_i(t) \geq \theta_i$, then agent i is considered ready for vaccination at time t. However, this readiness must be reconciled with the system's supply capacity. Let $V_t \subseteq \{i: E_i(t) = 1 \wedge VW_i(t) \geq \theta_i\}$ be the set of ready agents. Then, the subset of agents who actually receive the vaccine is given as follows:

$$V_t^{allocated} \subseteq V_t, \text{such that } \left|V_t^{allocated}\right| \leq V_{available}(t) \quad (19)$$

Allocation in V_t can be resolved using a selection mechanism, such as first-come-first-served, or queue priority based on risk scores or social centrality.

For each $i \in V_t^{allocated}$, the transition occurs as $X_i(t + 1) = V$. This mechanism ensures that vaccination is bounded by logistical realism and not only cognitive factors.

To represent time-varying vaccine availability, the supply curve $V_{available}(t)$ can be generated using a univariate ARIMA process or derived from real-world data. A simple ARIMA(1,1,1) model can be expressed as follows:

$$\Delta V_t = \phi \Delta V_{t-1} + \theta \varepsilon_{t-1} + \varepsilon_t \quad (20)$$

where $\Delta V_t = V_{available}(t) - V_{available}(t - 1)$ is the first difference in available doses; ϕ is the autoregressive coefficient; θ is the moving average coefficient; $\varepsilon_t \sim N(0, \sigma^2)$ is the white noise process.

This allows the simulation of dose delivery fluctuations, ramp-up periods, or supply chain disruptions. Alternative formulations, such as exponential growth or periodic shortages, can be used to encode scenario-based supply curves.

To simulate public health strategies, we define a dynamic priority set P_t to determine which agents are eligible for vaccination at each time step. Formally:

$$P_t = \{i \in \{1, .., N\} | X_i(t) = 1\} \quad (21)$$

where $X_i(t)$ is a binary eligibility flag computed using one or more of the following dimensions:

– risk score $r_i \geq 0$, based on age, comorbidities, or social exposure;

– sociological cluster C_i, to model targeted outreach or resistance;

– occupation class to simulate prioritization of health care workers;

– geographic location or network centrality for hotspot vaccination.

This design supports equity-driven, risk-minimizing, and resistance-countering policies. For example, a policymaker may prioritize conformists in early rounds or avoid skeptics initially due to high refusal probability.

The behavioural framework supports the integration of soft and hard policy interventions. Mandates are implemented by adjusting the decision threshold θ_i, effectively lowering the resistance to vaccination as follows:

$$\theta_i(t) = \theta_i - \Delta\theta \quad (22)$$

for $t \in T_{mandate}$, $i \in \Omega_{mandated}$.

Alternatively, public campaigns may increase the social influence score $SI_i(t)$ or alter the cluster-based coefficient $\phi(C_i)$, indirectly increasing vaccination willingness. For example:

$$SI_i(t + 1) = SI_i(t) + \Delta_{campaign} \quad (23)$$

This allows testing different communication strategies, such as mass media vs. targeted microcampaigns, and their relative impacts under supply-limited conditions.

While the baseline vaccination logic developed thus far assumes a single-dose paradigm with immediate immunity, real-world vaccination campaigns, especially those involving COVID-19 mRNA and vector-based vaccines, typically require multiple doses administered at specified time intervals, and immunity is known to build progressively rather than instantaneously. To incorporate these biological and logistical complexities, we introduce an extension to the vaccination model, including the dose count, immune lag, and immunity level.

Let each agent i be associated with a vaccine state tuple as follows:

ISSN 1814-4225 (print)
ISSN 2663-2012 (online)

$$V_i(t) = \left(V_i^{(k)}(t), \tau_i^{(k)}(t), \varepsilon_i(t)\right) \quad (24)$$

This tuple consists of three components. $V_i^{(k)}(t) \in \{0, 1, \ldots, K\}$ is the number of doses received by agent i up to time t, where K denotes the maximum required doses for full vaccination (e.g., K = 2 for Pfizer/Moderna, K = 1 for Johnson & Johnson). $\tau_i^{(k)}(t)$ is the elapsed time since the most recent dose, where $t^{(k)}$ is the timestamp of dose k. $\varepsilon_i(t) \in [0, 1]$ is the current effective immunity level, reflecting partial protection before the full immune response matures.

The effective immunity $\varepsilon_i(t)$ is modeled as a function of both the number of doses received and the time since the most recent dose:

$$\varepsilon_i(t) = \varepsilon_{max}\left(1 - e^{-\lambda_{imm}\tau_i^{(k)}(t)}\right)v_i(t) + \varepsilon_{partial}v_i. \quad (25)$$

This formulation distinguishes between two immunological regimes:

1. Full vaccination response. When the agent has received the complete dose schedule ($V_i^{(k)} = K$), their immunity increases over time $\tau_i^{(k)}$, governed by the rate constant λ_{imm}. The exponential form reflects the biological kinetics of antibody production and T-cell activation. The maximum attainable efficacy is denoted ε_{max}, typically between 0.85 and 0.95 for COVID-19 mRNA vaccines [29].

2. Partial immunity state. If the agent has received only one dose (i.e., $V_i^{(k)} = 1$ when K = 2), a constant partial efficacy $\varepsilon_{partial} \in [0.3, 0.7]$ is assigned. This value reflects the observed partial protection from severe disease or symptomatic infection. Behavioural consequences may also differ in this state (e.g., lower mask adherence) although this is addressed in subsequent iterations.

Upon meeting the eligibility criteria and expressing sufficient willingness, an agent receives their first dose, incrementing $V_i^{(k)} \leftarrow 1$ and setting $t^{(1)} = t$. The agent then enters a waiting state for the second dose, subject to a minimum interval constraint ΔT_{min}, representing the medically recommended dose spacing.

The second dose depend on both:

$$t - t^{(1)} \geq \Delta T_{min} \quad (26)$$

$$V_{available}(t) > 0 \quad (27)$$

If these conditions are satisfied, and the agent remains willing, then:

$$V_i^{(k)} \leftarrow 2, t^{(2)} = t, X_i(t+1) = V^{(2)} \quad (28)$$

The label $V^{(2)}$ denotes fully vaccinated agents in the epidemiological state machine. This enables conditional logic for infection resistance, mobility behaviour, or booster eligibility in future iterations.

In real-world campaigns, many individuals may fail to complete the full vaccine schedule because of forgetfulness, access barriers, misinformation, or changing risk perception. Let $\rho_{drop} \in [0, 1]$ denote the dropout probability, which can be stochastically assigned to agents following their first dose as follows:

$$P_{drop}(i) = \rho_{drop} + \alpha_M M_i(t) - \alpha_S SI_i(t) \quad (29)$$

where α_M and α_S are weights capturing how misinformation and social influence, respectively, modify dropout risk. This function simulates behaviorally grounded attrition, where skeptical or socially isolated agents are more likely to skip the second dose.

Agents who drop out remain partially vaccinated, with persistent $\varepsilon_i(t) = \varepsilon_{partial}$ and may never transition to full immunity. This extension is crucial for modelling under-vaccinated subpopulations and estimating the epidemiological consequences of incomplete coverage.

The vaccination state can be used to treat subsequent behavioural modules. For example, agents in state $V^{(1)}$ (partially vaccinated) or $V^{(2)}$ (fully vaccinated) may exhibit changes in contact rate (e.g., increased socialization), mask usage or risk avoidance, and information spread behaviour (e.g., confidence in correcting others).

These feedback effects may be modelled by modifying β_{ij} or behavioural parameters $SI_i(t)$, $M_i(t)$, and $VW_i(t)$ conditionally on $V_i(t)$.

4. Case Study

4.1. Setup and Model's Assumptions

To evaluate the capabilities of the proposed agent-based framework, a case study simulating the spread of a COVID-like infectious disease in a synthetic population was conducted. The simulation was executed over 120 days with a population of 1,000 agents. The model employs a discrete-time SEIRDV structure with compartmental state transitions updated at each time step.

The biological parameters were selected to reflect the average epidemiological characteristics of SARS-CoV-2 based on early-pandemic estimates. Vaccine-induced immunity was assumed to be immediate and effective, with no waning or breakthrough infections within the simulated period. Without behavioural resistance or misinformation, vaccination proceeded at a constant daily rate. Multiple scenarios with varying assumptions regarding vaccine uptake and belief evolution were conducted to isolate and compare the effects of behavioural and informational dynamics.

The parameter summary is presented in Table 5.

Table 5

Case study parameters

Parameter	Description	Value
N	Population size	1000
T	Duration of simulation	120 days
β	Transmission rate	0.002
σ	Incubation rate	1/5.2
γ	Recovery rate	1/10
μ	Daily mortality rate from infection	0.006
ε	Vaccine efficacy (probability of protection)	0.9 (90%)
v_{max}	Maximum daily vaccination rate (baseline)	1,5% of S
Initial conditions	[S, E, I, R, V, D] at t=0	[970, 20, 10, 0, 0, 0]
M(0)	Initial misinformation score	0.2
The growth rate of misinformation	Daily rate of increase in misinformation	0.2
Misinformation decay rate (intervention)	Daily reduction after countermeasures	-0.005
Day of Intervention	Day when counter-misinformation campaigns begin	Day 40

Each simulation scenario modifies specific behavioural components while maintaining consistent biological assumptions. The baseline case models optimal conditions with full willingness to vaccinate, while subsequent scenarios explore the implications of behavioural resistance (fixed hesitancy), misinformation-driven hesitancy (dynamic belief suppression), and corrective communication interventions (reversing misinformation growth). This structured progression enables the comparative evaluation of social-behavioral drivers within the same epidemiological framework.

All case study simulations were developed and executed in Python (v3.10), leveraging the NumPy and Matplotlib libraries for numerical operations and visualization. The simulation logic was implemented procedurally to maintain transparency in agent state transitions and subsystem interactions. Each compartmental state was updated iteratively using the deterministic update rules at each separate time step. The behavioural dynamics, including vaccination willingness and misinformation score evolution, were modelled using continuous variables governed by parameterized functions, enabling modular experimentation. The simulation outputs, including infection curves, vaccination coverage, mortality counts, and misinformation trajectories, were stored in Pandas DataFrames and exported for analysis. All plots were generated programmatically, ensuring reproducibility and alignment with the computational pipeline.

4.2. Baseline Dynamics

In the baseline scenario, agents readily accepted vaccination when eligible, and misinformation or behavioural hesitancy was not modelled. Under this assumption, the epidemic curve showed a moderate initial surge in infections, followed by a rapid decline due to increasing immunity in the population. The peak number of infectious cases occurred early, and cumulative mortality remained limited.

Vaccination coverage increased steadily throughout the simulation, surpassing 75% by day 120. This scenario serves as a control against which subsequent behaviorally constrained simulations can be compared (Fig. 3).

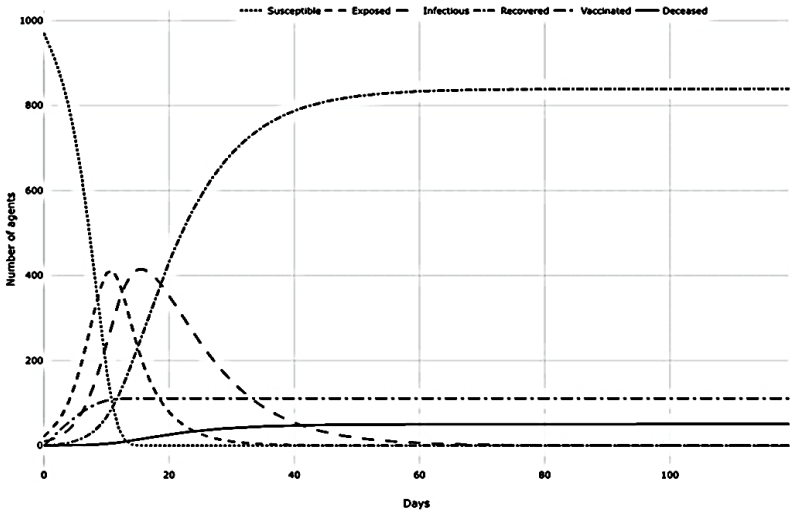

Figure 3. Baseline dynamics

ISSN 1814-4225 (print)
ISSN 2663-2012 (online)

4.3. Behavioural Resistance Scenario

To demonstrate behavioural resistance, fixed behavioural resistance by reducing the daily vaccination rate to 0.5% has been introduced, representing populations with intrinsic skepticism or logistical barriers to uptake. All other parameters remained unchanged. Figure 4 illustrates the impact of behavioural vaccine resistance on epidemic dynamics.

The results revealed a clear divergence from the baseline. The infectious curve peaked later and was higher, indicating delayed epidemic control. Total vaccination coverage remained below 50% at the end of the simulation, and cumulative deaths were nearly 50% higher than at baseline. This scenario highlights the vulnerability of public health outcomes when even modest resistance levels delay herd immunity.

4.4. Misinformation-Driven Vaccine Hesitancy

A time-dependent misinformation score $M(t) \in [0,1]$ was introduced to simulate dynamic behavioural feedback. This score increased gradually, starting from $M(0) = 0.2$ and grew according to an exponential saturation function. The daily vaccination rate was defined as:

$$v(t) = v_{max} \cdot (1 - M(t)) \quad (30)$$

where $v_{max} = 0.015$. This relationship demonstrates how increasing misinformation exposure suppresses vaccination willingness in the population (Fig. 5).

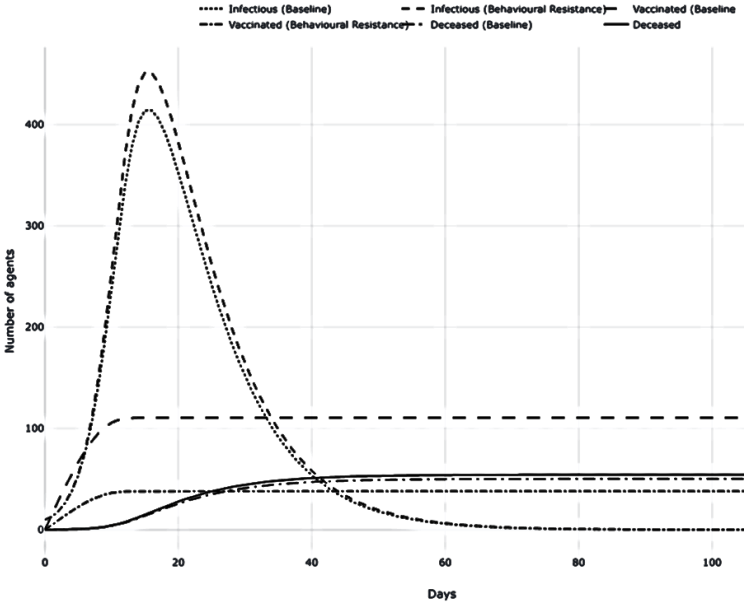

Figure 4. Impact of behavioural vaccine resistance

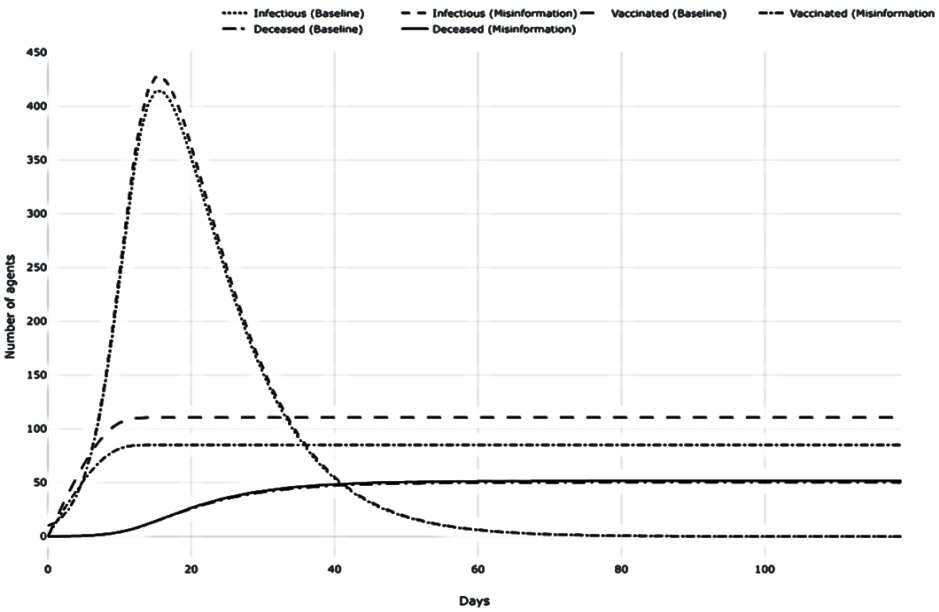

Figure 5. Misinformation-driven vaccine hesitancy

The simulation results showed that as M(t) rose, the vaccine uptake declined, falling far below the baseline. Infectious cases peaked significantly higher than in the behavioural resistance scenario, and the accumulated deaths were accelerated. By day 120, total vaccination coverage reached only ~500 individuals, underscoring how real-time information dynamics can critically undermine epidemic containment.

4.5. Counter-Misinformation Intervention

A counter-misinformation intervention was introduced into the simulation framework to evaluate the effectiveness of corrective communication strategies. The intervention began on day 30 and modelled a decline in the population-wide misinformation score M(t) over time, representing the effects of public messaging campaigns, trust-building efforts, and content moderation by health authorities or platforms. Concurrently, the daily vaccination rate was set to 3% of the susceptible population, allowing for a more responsive public health effort under reduced belief suppression (Fig. 6).

The simulation results demonstrate visible improvements compared to the misinformation-only scenario. As the misinformation score decreased, vaccine uptake increased, leading to earlier containment of the infectious peak and a steeper reduction in active cases. By the end of the simulation, more than 700 individuals had been vaccinated, and cumulative mortality was notably reduced. These findings reinforce the notion that information interventions can produce system-level effects by reshaping belief trajectories and restoring public compliance with health guidance. This scenario highlights the importance of integrating communication strategies into epidemic planning, especially when trust in vaccination is vulnerable to sustained disinformation exposure.

4.6. Comparative Summary

Across all four scenarios, outcomes varied significantly depending on the presence and nature of vaccine hesitancy (Table 6).

Table 6

Summary of the experimental study

Scenario	Peak infectious	Final vaccinated	Total deaths
Baseline	Low	High (750)	Low
Behavioural resistance	Moderate	Low (480)	Moderate
Misinformation-driven hesitancy	High	Low (500)	High
Enhanced counter-misinformation	Moderate	Moderate (700)	Moderate

These case studies demonstrate how social behaviour and information dynamics are not peripheral to epidemic modelling but are, in fact, central drivers of system outcomes. Integrating these behavioural mechanisms into simulation frameworks enhances predictive models' realism and policy relevance.

5. Discussion

This study presents a novel, theoretically grounded agent-based framework that integrates multiple subsystems to simulate infectious disease dynamics in the context of vaccine hesitancy and health-related misinformation.

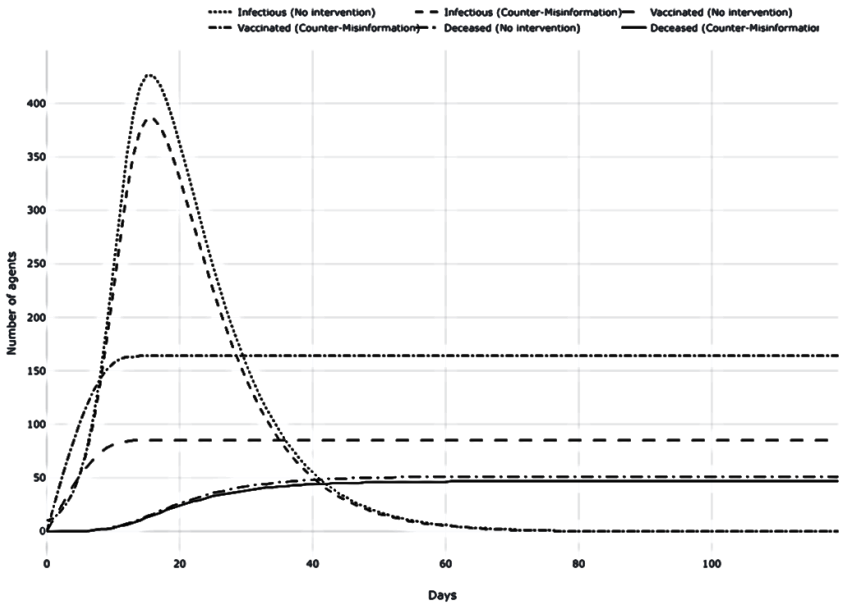

Figure 6. Effect of Counter-Misinformation Campaign

ISSN 1814-4225 (print)
ISSN 2663-2012 (online)

Unlike traditional epidemiological models, which typically abstract individual decision-making into aggregate parameters, the proposed model explicitly accounts for micro-level cognitive states, social influence mechanisms, and structural constraints on vaccination. This design enhances the explanatory power and policy relevance of epidemic simulations, especially in socially and behaviorally heterogeneous populations.

A defining feature of this framework is its incorporation of misinformation propagation as an endogenous cognitive state that evolves through peer interactions and exogenous media inputs. This finding aligns with recent empirical work highlighting the causal impact of misinformation on vaccination intentions and health behaviours during the COVID-19 pandemic [30-31]. Although several models have represented misinformation as a static parameter [23], the current approach models belief dynamics through memory decay, social susceptibility, and targeted disinformation shocks. This allows the emergence of structural phenomena such as echo chambers [32], belief polarization, and informational resilience, all of which shape downstream behavioural patterns and epidemic trajectories.

The model also introduces agent-level heterogeneity in vaccination willingness, which is rooted in the sociological typologies of belief and trust. This cognitive-behavioural representation supports the simulation of bounded rationality, risk perception, and social learning, all critical determinants of vaccine uptake identified in behavioural studies [33]. The decision-making architecture, which is based on individual thresholds and time-varying motivation, builds on social diffusion theory and decision inertia models [34], and allows for the observation of group-level hesitancy clustering and delayed vaccine adoption, which have been empirically reported in several countries during the COVID-19 rollout [35].

From a structural perspective, the vaccination logistics subsystem distinguishes this model from prior agent-based models by incorporating supply-side constraints, eligibility policies, and dropout probabilities. These features are crucial for simulating the real-world divergence between vaccine willingness and access, as highlighted in global distribution studies [36, 37]. Using ARIMA models to simulate time-varying vaccine availability introduces stochastic realism to rollout scenarios, supporting the evaluation of dynamic policy interventions, such as phased prioritization or contingency planning for supply disruptions.

Several previous studies have validated the relevance of including the social context in epidemic models. The proposed framework operationalized these recommendations by integrating a behavioural subsystem calibrated with agent typologies and dynamic belief formation. Unlike models with fixed parameters for vaccine acceptance or compliance (e.g., [16, 18]), this model allows agents to adapt based on evolving norms, peer behaviour, and exposure to competing narratives.

The model architecture supports modular experimentation, interpretability, and extensibility. Subsystems are loosely coupled yet dynamically interdependent, enabling the testing of targeted interventions and complex feedback effects. For example, misinformation campaigns can be simulated as exogenous shocks, and their impact can be traced to changes in belief scores, social pressure, and resulting vaccination behaviour. This capacity is critical when evaluating communication strategies, such as nudging interventions or corrective information targeting specific sociological clusters [38].

The case study simulations presented in this paper provide critical insights into how the interplay of behavioural resistance, misinformation exposure, and communication interventions can shape epidemic trajectories. The findings underscore that even modest declines in vaccination willingness, whether static or dynamically induced by rising misinformation, can significantly alter the course of an outbreak. In the behavioural resistance scenario, in which vaccine uptake was artificially capped at 0.5% of the susceptible population per day, the infectious peak was delayed and amplified. Total mortality increased by over 40% from baseline. These results parallel empirical findings from countries with high vaccine hesitancy, where persistent refusal contributed to prolonged transmission and avoidable hospitalizations [39, 40].

More critically, the misinformation-driven scenario highlighted the cascading effects of belief dynamics on population-level outcomes. As misinformation scores rose, willingness to vaccinate decreased nonlinearly, resulting in a higher and sustained infectious burden. These findings echo evidence from longitudinal studies that linked social media exposure to lower vaccine intent [31], particularly COVID-19 conspiracy theories and politicized discourse [30]. The model operationalized these dynamics via a feedback loop between belief exposure, social influence, and vaccination decisions, allowing for emergent properties such as delayed herd immunity and sustained vulnerability in information-resistant subpopulations.

The counter-misinformation intervention scenario demonstrated that belief trajectories are not fixed and that well-timed corrective strategies can meaningfully shift system dynamics. A modest, mid-simulation reduction in misinformation growth yielded faster epidemic suppression and a marked reduction in mortality. This finding aligns with recent experimental studies showing that factual corrections from trusted sources can increase vaccine intent, particularly when targeted at hesitant groups [41, 42]. These findings reinforce the importance of strategic communication planning as a core component of epidemic response, not merely an auxiliary to biomedical measures.

The simulations also suggest that timing matters. Interventions deployed too late may diminish returns if misinformation exposure has already eroded public trust. Therefore, real-world efforts to counter misinformation must focus on content accuracy, timeliness, source credibility, and network penetration. Emerging tools, such as pre-bunking, inoculation theory, and algorithmic throttling of false content, offer promising avenues for policy and platform design [43].

This case study reinforces the central proposition of the model: that information is an epidemic in itself, that travels through social networks, shapes behaviour, and alters biological outcomes. In a context in which pandemics are increasingly shaped by both pathogens and platforms, integrating behavioural and informational subsystems into epidemic modelling is not only theoretically justified but also practically imperative.

Despite these contributions, the proposed model has several limitations. First, the current version assumes a static contact network, which may not reflect real-time behavioural adaptation (e.g., reduced mobility or voluntary isolation). Incorporating temporal contact patterns (e.g., activity-based or mobility-informed networks) would improve alignment with empirical mobility studies, such as those using SafeGraph or Google Community Mobility Reports. Second, the model assumes homogeneous biological parameters across agents (e.g., uniform progression rates and mortality risk). Stratifying these by age, comorbidity, or socio-economic status would improve predictive fidelity. Third, while the model formalizes belief propagation and vaccine decisions, it has not yet been calibrated using empirical surveys or social media data. This direction is important for future validation and scenario realistic modelling.

This study advances the theoretical foundations of agent-based infectious disease modelling by integrating behavioural science, cognitive modelling, and logistical realism. The proposed framework captures the interplay among misinformation, belief dynamics, and public health interventions within a unified epidemic system. This study builds on and extends recent literature (e.g., [6, 21, 17]), offering a powerful tool for exploring behavioural epidemiology under uncertainty. As societies are increasingly exposed to digital misinformation, integrative models are essential for designing responsive, equitable, evidence-based health strategies.

7. Conclusions

This paper presents a novel theoretical framework for agent-based modelling of infectious disease spread that captures the multi-layered dynamics of epidemiological transmission, behavioural decision-making and information diffusion. The proposed model addresses critical gaps in existing simulation approaches by incorporating belief-driven vaccination behaviour, misinformation propagation, vaccine supply constraints and policy interventions. The architecture emphasizes modularity, enabling targeted experimentation with each subsystem while maintaining coherence in emergent population-level outcomes.

This work's scientific novelty lies in its integration of cognitive and informational dimensions into epidemic modelling. Unlike conventional agent-based models, which often treat vaccine acceptance and misinformation as static parameters, this model conceptualizes them as dynamic, socially embedded processes shaped by peer influence, exogenous media events, and evolving belief states. The behavioural subsystem introduces adaptive agents whose vaccination decisions respond to social pressure, perceived risks and misinformation exposure. This theoretical contribution provides a foundation for studying how socio-cognitive structures mediate epidemiological trends.

The results of the case study simulations underscore the model's practical relevance. The scenarios demonstrated that even modest behavioural resistance or increasing misinformation can delay epidemic control and increase cumulative mortality. When belief dynamics are explicitly modeled, vaccine uptake becomes a function of social context and narrative exposure rather than an exogenous assumption. Introducing a counter-misinformation campaign in the simulation, implemented through a declining belief score, resulted in higher vaccination coverage and reduced peak infectious burden. These findings validate the importance of information-based interventions and demonstrate the model's potential to support communication strategy design, particularly for volatile public trust.

Practically, the framework serves as a flexible decision-support tool for public health planning, particularly in contexts where misinformation or vaccine hesitancy undermines the effectiveness of interventions. It can be adapted for scenario analysis of communication strategies, policy prioritization, and targeted resource allocation under uncertainty. The explicit inclusion of vaccine logistics and behavioural drop-out also enhances their utility for planning real-world rollouts that involve multi-dose regimes, limited supply, and fluctuating public trust.

Future research will focus on empirical calibration and validation of the model using real-world data sources, such as epidemiological statistics, survey-based vaccine attitudes, and social media misinformation trends. Integrating dynamic contact networks based on mobility patterns or daily activities can further increase the realistic perception of behavioural adaptation and transmission pathways. In addition, extending the belief propagation module to include counter-misinformation campaigns, nudging interventions, or trust dynamics in

ISSN 1814-4225 (print)
ISSN 2663-2012 (online)

information sources would enable more precise modelling of communication effects. Applying the framework to different sociopolitical contexts and other infectious diseases, such as monkeypox and influenza, represents another promising direction. Finally, embedding the model in a participatory simulation platform could enhance its use in collaborative policy design and stakeholder engagement.

Conflict of interest

The author declare that they have no conflict of interest concerning this research, whether financial, personal, authorship, or otherwise, that could affect the research and its results presented in this paper.

Funding

The study was funded by the National Research Foundation of Ukraine in the framework of the research project 2023.03/0197 on the topic *"Multidisciplinary study of the impact of emergency situations on the infectious diseases spreading to support management decision-making in the field of population biosafety"*.

Use of Artificial Intelligence

Generative AI tools (Grammarly, ChatGPT 4o) have been used for grammar checks and text polishing.

The author has read and agreed to the published version of this manuscript.

References

1. Kermack, W.O., & McKendrick, A.G. A Contribution to the Mathematical Theory of Epidemics. *Proceedings of the Royal Society of London. Series A, Containing Papers of a Mathematical and Physical Character*, 1927, vol. 115, pp. 700–721.

2. Gatto, A., Accarino, G., Aloisi, V., Immorlano, F., Donato, F., & Aloisio, G. Limits of Compartmental Models and New Opportunities for Machine Learning: A Case Study to Forecast the Second Wave of COVID-19 Hospitalizations in Lombardy, Italy. *Informatics*, 2021, vol. 8, article no. 57. DOI: 10.3390/informatics8030057.

3. Tracy, M., Cerdá, M., & Keyes, K. M. Agent-Based Modeling in Public Health: Current Applications and Future Directions. *Annual Review of Public Health*, 2018, vol. 39, pp. 77–94. DOI: 10.1146/annurev-publhealth-040617-014317.

4. Wang, P., Zheng, X., & Liu, H. Simulation and Forecasting Models of COVID-19 Taking into Account Spatio-Temporal Dynamic Characteristics: A Review. *Frontiers in Public Health*, 2022, vol. 10, article no. 1033432. DOI: 10.3389/fpubh.2022.1033432.

5. Fair, K.R., Karatayev, V. A., Anand, M., & Bauch, C. T. Estimating COVID-19 Cases and Deaths Prevented by Non-Pharmaceutical Interventions, and the Impact of Individual Actions: A Retrospective Model-Based Analysis. *Epidemics*, 2022, vol. 39, article no. 100557. DOI: 10.1016/j.epidem.2022.100557.

6. Kerr, C. C., Stuart, R. M., Mistry, D., Abeysuriya, R. G., Rosenfeld, K., Hart, G. R., Núñez, R. C., Cohen, J. A., Selvaraj, P., Hagedorn, B., & et al. Covasim: An Agent-Based Model of COVID-19 Dynamics and Interventions. *PLOS Computational Biology*, 2021, vol. 17, article no. e1009149. DOI: 10.1371/journal.pcbi.1009149.

7. do Nascimento, I. J. B., Pizarro, A. B., Almeida, J., Azzopardi-Muscat, N., Gonçalves, M. A., Björklund, M., & Novillo-Ortiz, D. Infodemics and Health Misinformation: A Systematic Review of Reviews. *Bulletin of the World Health Organization*, 2022, vol. 100, pp. 544–561. DOI: 10.2471/blt.21.287654.

8. Briand, S.C., Cinelli, M., Nguyen, T., Lewis, R., Prybylski, D., Valensise, C.M., Colizza, V., Tozzi, A.E., Perra, N., Baronchelli, A., & et al. Infodemics: A New Challenge for Public Health. *Cell*, 2021, vol. 184, pp. 6010–6014. DOI: 10.1016/j.cell.2021.10.031.

9. van der Linden, S. Misinformation: Susceptibility, Spread, and Interventions to Immunize the Public. *Nature Medicine*, 2022, vol. 28, pp. 460–467. DOI: 10.1038/s41591-022-01713-6.

10. Zakharchenko, O., Avramenko, R., Zakharchenko, A., Korobchuk, A., Fedushko, S., Syerov, Y., & Trach, O. Multifaceted Nature of Social Media Content Propagating COVID-19 Vaccine Hesitancy: Ukrainian Case. *Procedia Computer Science*, 2022, vol. 198, pp. 682–687. DOI: 10.1016/j.procs.2021.12.306.

11. Mochurad, L., Dereviannyi, A., & Antoniv, U. Classification of X-Ray Images of the Chest Using Convolutional Neural Networks. *CEUR Workshop Proceedings*, 2021, vol. 3038, pp. 269–282.

12. Izonin, I., Tkachenko, R., Yemets, K., & Havryliuk, M. An Interpretable Ensemble Structure with a Non-Iterative Training Algorithm to Improve the Predictive Accuracy of Healthcare Data Analysis. *Scientific Reports*, 2024, vol. 14, article no. 12947. DOI: 10.1038/s41598-024-61776-y.

13. Nitzsche, C., & Simm, S. Agent-Based Modeling to Estimate the Impact of Lockdown Scenarios and Events on a Pandemic Exemplified on SARS-CoV-2. *Scientific Reports*, 2024, vol. 14, article no. 13391. DOI: 10.1038/s41598-024-63795-1.

14. Chumachenko, D., Bazilevych, K., Butkevych, M., Meniailov, I., Parfeniuk, Y., Sidenko, I., & Chumachenko, T. Methodology for Assessing the Impact of Emergencies on the Spread of Infectious Diseases. *Radioelectronic and Computer Systems*, 2024, vol. 2024, iss. 3, pp. 6–26. DOI: 10.32620/reks.2024.3.01.

15. Rosenstrom, E. T., Ivy, J. S., Mayorga, M. E., & Swann, J. L. COVSIM: A Stochastic Agent-Based COVID-19 SIMulation Model for North Carolina. *Epidemics*, 2024, vol. 46, article no. 100752. DOI: 10.1016/j.epidem.2024.100752.

16. Nemiche, M., Timouyas, M., Regragui, Y., & Bezza, H. Dynamic Agent-Based Model for COVID-19 Epidemic Spread Using Social Network Information.

Lecture Notes in Networks and Systems, 2024, vol. 905, pp. 436–445. DOI: 10.1007/978-3-031-52385-4_42.

17. Ebrahimi, A. H., Alesheikh, A. A., Hooshangi, N., Sharif, M., & Mollalo, A. Modeling COVID-19 Transmission in Closed Indoor Settings: An Agent-Based Approach with Comprehensive Sensitivity Analysis. *Information*, 2024, vol. 15, article no. 362. DOI: 10.3390/info15060362.

18. Cuevas, E. An Agent-Based Model to Evaluate the COVID-19 Transmission Risks in Facilities. *Computers in Biology and Medicine*, 2020, vol. 121, article no. 103827. DOI: 10.1016/j.compbiomed.2020.103827.

19. Najmi, A., Nazari, S., Safarighouzhdi, F., Miller, E.J., MacIntyre, R., & Rashidi, T. H. Easing or Tightening Control Strategies: Determination of COVID-19 Parameters for an Agent-Based Model. *Transportation*, 2021, vol. 49, pp. 1265–1293. DOI: 10.1007/s11116-021-10210-7.

20. Gostoli, U., Silverman, E. Self-Isolation and Testing Behaviour during the COVID-19 Pandemic: An Agent-Based Model. *Artificial Life*, 2023, vol. 29, pp. 94–117. DOI: 10.1162/artl_a_00392.

21. Qiao, Q., Cheung, C., Yunusa- Kaltungo, A., Manu, P., Cao, R., & Yuan, Z. An Interactive Agent-Based Modelling Framework for Assessing COVID-19 Transmission Risk on Construction Site. *Safety Science*, 2023, vol. 168, article no. 106312. DOI: 10.1016/j.ssci.2023.106312.

22. Olszewski, R., Palka, P., & Wendland, A. Agent-Based Modeling as a Tool for Predicting the Spatial-Temporal Diffusion of the COVID-19 Pandemic. *2021 IEEE International Conference on Industrial Engineering and Engineering Management (IEEM) 2021*, 2021, pp. 11–15. DOI: 10.1109/ieem50564.2021.9672878.

23. Bhattacharya, P., Machi, D., Chen, J., Hoops, S., Lewis, B., Mortveit, H., Venkatramanan, S., Wilson, M. L., Marathe, A., Porebski, P., & et al. AI-Driven Agent-Based Models to Study the Role of Vaccine Acceptance in Controlling COVID-19 Spread in the US. *2021 IEEE International Conference on Big Data (Big Data)*, 2021, pp. 1566–1574. DOI: 10.1109/bigdata52589.2021.9671811.

24. Bongolan, V. P., Ang, K. K., Celeste, J. J., Minoza, J. M., Caoili, S., Rivera, R. L., de Castro, R. COVID-19 Agent-Based Model: An Epidemiological Simulator Applied in Vaccination Scenarios for Quezon City, Philippines. *The international archives of the photogrammetry, remote sensing and spatial information sciences*, 2021, pp. 65–70. DOI: 10.5194/isprs-archives-xlvi-4-w6-2021-65-2021.

25. Kissler, S. M., Tedijanto, C., Goldstein, E., Grad, Y. H., & Lipsitch, M. Projecting the Transmission Dynamics of SARS-CoV-2 through the Postpandemic Period. *Science*, 2020, vol. 368, pp. 860–868. DOI: 10.1126/science.abb5793.

26. Lauer, S. A., Grantz, K. H., Bi, Q., Jones, F. K., Zheng, Q., Meredith, H. R., Azman, A. S., Reich, N. G., Lessler, J. The Incubation Period of Coronavirus Disease 2019 (COVID-19) from Publicly Reported Confirmed Cases: Estimation and Application. *Annals of Internal Medicine*, 2020, vol. 172, pp. 577–582. DOI: 10.7326/M20-0504.

27. Mohammed, I., Nauman, A., Paul, P., Ganesan, S., Chen, K.-H., Jalil, S. M. S., Jaouni, S. H., Kawas, H., Khan, W. A., Vattoth, A. L., & et al. The Efficacy and Effectiveness of the COVID-19 Vaccines in Reducing Infection, Severity, Hospitalization, and Mortality: A Systematic Review. *Human Vaccines & Immunotherapeutics*, 2022, vol. 18, article no. 2027160. DOI: 10.1080/21645515.2022.2027160.

28. Chumachenko, D., Chumachenko, T., Kirinovych, N., Meniailov, I., Muradyan, O., Salun, O. Barriers of COVID-19 Vaccination in Ukraine during the War: The Simulation Study Using ARIMA Model. *Radioelectronic and Computer Systems*, 2022, vol. 2022, iss. 3, pp. 20–32. DOI: 10.32620/reks.2022.3.02.

29. Zheng, C., Shao, W., Chen, X., Zhang, B., Wang, G., Zhang, W. Real-World Effectiveness of COVID-19 Vaccines: A Literature Review and Meta-Analysis. *International Journal of Infectious Diseases*, 2022, vol. 114, pp. 252–260. DOI: 10.1016/j.ijid.2021.11.009.

30. Loomba, S., de Figueiredo, A., Piatek, S.J., de Graaf, K., & Larson, H. J. Measuring the Impact of COVID-19 Vaccine Misinformation on Vaccination Intent in the UK and USA. *Nature Human Behaviour*, 2021, vol. 5, pp. 337–348. DOI: 10.1038/s41562-021-01056-1.

31. Roozenbeek, J., Schneider, C. R., Dryhurst, S., Kerr, J., Freeman, A. L. J., Recchia, G., van der Bles, A.M., & van der Linden, S. Susceptibility to Misinformation about COVID-19 around the World. *Royal Society Open Science*, 2020, vol. 7, article no. 201199. DOI: 10.1098/rsos.201199.

32. Cinelli, M., Morales, G. D. F., Galeazzi, A., Quattrociocchi, W., & Starnini, M. The Echo Chamber Effect on Social Media. *Proceedings of the National Academy of Sciences*, 2021, vol. 118, article no. e2023301118. DOI: 10.1073/pnas.2023301118.

33. Betsch, C., Schmid, P., Heinemeier, D., Korn, L., Holtmann, C., & Böhm, R. Beyond Confidence: Development of a Measure Assessing the 5C Psychological Antecedents of Vaccination. *PLOS ONE*, 2018, vol. 13, article no. e0208601. DOI: 10.1371/journal.pone.0208601.

34. Centola, D., Becker, J., Brackbill, D., & Baronchelli, A. Experimental Evidence for Tipping Points in Social Convention. *Science*, 2018, vol. 360, pp. 1116–1119. DOI: 10.1126/science.aas8827.

35. de Figueiredo, A., & Larson, H.J. Exploratory Study of the Global Intent to Accept COVID-19 Vaccinations. *Communications Medicine*, 2021, vol. 1, article no. 30. DOI: 10.1038/s43856-021-00027-x.

36. Acharya, K. P., Ghimire, T. R., & Subramanya, S.H. Access to and Equitable Distribution of COVID-19 Vaccine in Low-Income Countries. *Npj Vaccines*, 2021, vol. 6, article no. 54. DOI: 10.1038/s41541-021-00323-6.

ISSN 1814-4225 (print)
ISSN 2663-2012 (online)

37. Burki, T. Equitable Distribution of COVID-19 Vaccines. *The Lancet Infectious Diseases*, 2021, vol. 21, pp. 33–34. DOI: 10.1016/s1473-3099(20)30949-x.

38. Pennycook, G., McPhetres, J., Zhang, Y., Lu, J. G., Rand, D. G. Fighting COVID-19 Misinformation on Social Media: Experimental Evidence for a Scalable Accuracy-Nudge Intervention. *Psychological Science*, 2020, vol. 31, pp. 770–780. DOI: 10.1177/0956797620939054.

39. Lin, C., Tu, P., & Beitsch, L.M. Confidence and Receptivity for COVID-19 Vaccines: A Rapid Systematic Review. *Vaccines*, 2020, vol. 9, article no. 16. DOI: 10.3390/vaccines9010016.

40. Murphy, J., Vallières, F., Bentall, R.P., Shevlin, M., McBride, O., Hartman, T.K., McKay, R., Bennett, K., Mason, L., Gibson-Miller, J., & et al. Psychological Characteristics Associated with COVID-19 Vaccine Hesitancy and Resistance in Ireland and the United Kingdom. *Nature Communications*, 2021, vol. 12, article no. 29. DOI: 10.1038/s41467-020-20226-9.

41. Nyhan, B., & Reifler, J. The Roles of Information Deficits and Identity Threat in the Prevalence of Misperceptions. *Journal of Elections, Public Opinion and Parties*, 2018, vol. 29, pp. 222–244. DOI: 10.1080/17457289.2018.1465061.

42. Vraga, E. K., & Bode, L. Correction as a Solution for Health Misinformation on Social Media. *American Journal of Public Health*, 2020, vol. 110, pp. S278–S280. DOI: 10.2105/ajph.2020.305916.

43. van der Linden, S., Roozenbeek, J., & Compton, J. Inoculating against Fake News about COVID-19. *Frontiers in Psychology*, 2020, vol. 11, article no. 566790. DOI: 10.3389/fpsyg.2020.566790.

Received 24.11.2024, Accepted 17.02.2025

ТЕОРЕТИЧНИЙ ФРЕЙМВОРК АГЕНТНО-ОРІЄНТОВАНОГО МОДЕЛЮВАННЯ ДИНАМІКИ ІНФЕКЦІЙНИХ ХВОРОБ В УМОВАХ МІСІНФОРМАЦІЇ ТА ВАГАНЬ ЩОДО ВАКЦИНАЦІЇ

Д. І. Чумаченко

Актуальність цього дослідження зумовлена зростаючим значенням моделювання не лише біологічної передачі інфекційних хвороб, але й поведінкових та інформаційних чинників, що формують динаміку епідемій у реальному світі. Предметом дослідження є розробка агентно-орієнтованого фреймворку, здатного відображати складні взаємозв'язки між епідеміологічними процесами, поведінкою щодо вакцинації та поширенням місінформації. Мета дослідження: запропонувати та оцінити модульну, теоретично обґрунтовану модель, що імітує поширення інфекції з урахуванням прийняття рішень на основі переконань та впливу соціального оточення. Для досягнення цієї мети було поставлено такі завдання: проаналізувати сучасний стан агентно-орієнтованого моделювання епідемій, формалізувати архітектуру системи з когнітивними та логістичними підсистемами, а також провести симуляційні сценарії для дослідження впливу дезінформації та поведінкового опору на рівень вакцинації та динаміку епідемії. Методологія базується на дискретно-часовій структурі SEIRDV, розширеній агентними станами переконань, механізмами соціального впливу та динамічними рішеннями про вакцинацію. Модель була реалізована мовою Python та протестована через кейс-дослідження, що симулює спалах інфекції, подібної до COVID-19, у синтетичному населенні. Результати демонструють, що навіть помірний поведінковий опір може суттєво підвищити смертність і затримати контроль над епідемією, тоді як втручання проти дезінформації, за умови їх своєчасного та інтенсивного застосування, можуть підвищити охоплення вакцинацією і зменшити епідемічний тягар. У дослідженні зроблено висновок, що інтеграція поведінкової та інформаційної динаміки в моделі епідемій забезпечує більш реалістичний та релевантний інструмент аналізу комунікаційних стратегій, сценаріїв вакцинації та заходів охорони здоров'я в умовах невизначеності.

Ключові слова: епідемічна модель; епідемічний процес; моделювання епідемії; моделювання; агентно-орієнтоване моделювання, місінформація, вакцинальна неохота.

Чумаченко Дмитро Ігорович – канд. техн. наук, доц., доц. каф. математичного моделювання та штучного інтелекту, Національний аерокосмічний університет «Харківський авіаційний інститут», Харків, Україна; афілійований дослідник з лабораторією всюдисущих технологій охорони здоров'я, Університет Вотерлу, Вотерлу, Онтаріо, Канада; запрошений науковий співробітник, Школа міжнародних відносин Балсіллі, Вотерлу, Онтаріо, Канада.

Dmytro Chumachenko – PhD, Associate Professor, Associate Professor at the Department of Mathematical Modelling and Artificial Intelligence, National Aerospace University "Kharkiv Aviation Institute", Kharkiv, Ukraine; Research Affiliate with Ubiquitous Health Technology Lab, University of Waterloo, Waterloo, ON, Canada; Visiting Scholar, Balsillie School of International Affairs, Waterloo, ON, Canada.
e-mail: dichumachenko@gmail.com, ORCID: 0000- 0003-2623-3294.